Limnetica, 38(2): 555-573 (2019). DOI: 10.23818/limn.38.32

Dissolved organic matter variability along an impacted intermittent Mediterranean river

Verónica Granados* and Andrea Butturini

Departament de Biologia Evolutiva, Ecologia i Ciències Ambientals, Universitat de Barcelona, Diagonal 643, 08028 Barcelona, Spain.

* Corresponding author: v.granados@ub.edu

Received: 21/12/17 Accepted: 11/06/18

ABSTRACT

Dissolved organic matter variability along an impacted intermittent Mediterranean river

Hydrological variability is the key factor that modulates allochthonous inputs and in-river biotic processes and, thereby, the fate of dissolved organic matter (DOM) in rivers. However, little is known about how these factors, combined, change DOM quantity and quality along river courses.

This study explored how DOM quantity (in terms of dissolved organic carbon – DOC) and quality (in terms of optical properties) varied along a Mediterranean river, under contrasting hydrological conditions: drought and high flow. The study was performed in the Matarranya river, a system severely affected by water abstraction for agricultural irrigation and inputs of untreated residual waters.

DOM properties changed according to hydrology. DOM under high flow conditions was more terrigenous, humified, aromatic, and degraded and the concentration gradually increased downriver. In contrast, DOM was less degraded and more aliphatic under drought conditions. DOM spatial variability under drought and high flow conditions revealed that hydrology has a greater impact on DOM quality in headwaters than at downriver sites. Longitudinal changes in DOM were more evident under drought conditions. For instance, a longitudinal depletion of DOC, together with a decrease of the fresh DOM pool, was observed in a large fluvial segment (35 km long) that does not receive any notable anthropogenic inputs. In contrast, the contribution of the most aromatic and humified DOM pool was significantly higher downriver. This study confirms the role of hydrology as a main driver of DOM dynamics. Additionally, it shows that hydrological variability does not impact DOM properties uniformly along the river continuum. On the contrary, DOM properties are more sensitive to hydrological changes in headwaters than in downriver reaches.

Key words: Dissolved organic matter (DOM), river continuum concept (RCC), intermittent stream, hydrological variability, DOM dynamics, DOM optical properties, chemostasis

RESUMEN

Variabilidad de la materia orgánica disuelta a lo largo de un río mediterráneo impactado intermitentemente

La variabilidad hidrológica es el factor clave que modula las entradas alóctonas y los procesos bióticos en el río y, por lo tanto, el destino de la materia orgánica disuelta (MOD) en los ríos. Sin embargo, poco se sabe acerca de cómo estos factores combinados cambian la MOD y la calidad a lo largo de los cursos fluviales.

Este estudio explora cómo la cantidad de MOD (en términos de carbono orgánico disuelto - COD) y calidad (en términos de propiedades ópticas) varía a lo largo de un río mediterráneo, bajo condiciones hidrológicas opuestas: sequía (caudal muy bajo) y caudal alto. El estudio se realizó en el río Matarranya, un sistema severamente afectado por la extracción de agua para riego agrícola y aportes puntuales de aguas residuales no tratadas.

Las propiedades de la MOD cambiaron de acuerdo con la hidrología. La MOD bajo condiciones de caudal alto era más terrígena, humificada, aromática, degradada y la concentración aumentaba gradualmente aguas abajo. Por el contrario, la MOD estaba menos degradada y más alifática en condiciones de sequía. La variabilidad espacial de la MOD bajo condiciones de sequía y caudal alto reveló que la hidrología afecta la calidad de la MOD, siendo más severa en la cabecera que en el tramo *final del río. Los cambios longitudinales de la MOD fueron más evidentes en condiciones de sequía. Por ejemplo, en un segmento fluvial que no recibe ninguna aportación antropogénica notable (con 35 km de extensión), se observó una reducción de COD a largo del eje longitudinal, junto con una disminución de la MOD menos degradada. Por el contrario, la contribución de la MOD más aromática y humificada aumentó significativamente río abajo. Este estudio confirmó a la hidrología como impulsora principal de la dinámica de la MOD. Además, se evidencia que la variabilidad hidrológica no afecta a las propiedades de MOD uniformemente a lo largo del continuo fluvial. Por el contrario, las propiedades de MOD son más sensibles a los cambios hidrológicos en la cabecera que en curso bajo del río.*

Palabras clave: *Materia orgánica disuelta, concepto de río continuo, río intermitente, variabilidad hidrológica, dinámicas del MOD, propiedades ópticas del MOD, quimio-homeostasis*

INTRODUCTION

Dissolved organic matter (DOM) is a complex mixture of soluble organic compounds that vary in their reactivity and ecological role (Fellman *et al.*, 2010) DOM includes complex, polymeric compounds (humic and fulvic substances) as well as simple, well-defined molecules (sugars, proteins, lipids, organic acids, phenols, alcohols, among others). The molecular weights of DOM compounds rang from less than 100 to over 300 000 Daltons (Hayase & Tsubota, 1985; Thurman, 1985). These compounds can originate from terrestrial or aquatic sources as well as from anthropogenic inputs, such as treated and untreated wastewater effluents (Leenheer, 2009). DOM plays an important role in aquatic food webs, because it supplies energy, carbon (Wetzel, 1992) and nitrogen (Keil & Kirchman, 1991) for the heterotrophic community. However, the extent to which the dissolved organic compounds are metabolized in freshwater ecosystems depends on their biochemical composition (Benner, 2003). In freshwater ecosystems, DOM represents approximately 25 % of the total carbon transported downriver (Schlesinger & Melack, 1981; Meybeck, 1982) and its transport, reactivity and fate along fluvial courses is the product of internal (autochthonous) transformation processes and external (allochthonous) inputs from tributaries, occasional anthropogenic outlets (e.g., wastewater treatment plants, industries and urban settlements) and diffuse inputs from groundwater. The quantity and quality of allochthonous DOM inputs are strongly modulated by hydrology and, especially, the occurrence of extreme episodes such as droughts and floods (Buffam *et al.*, 2001; Butturini *et al.*, 2016).

Longitudinal DOM dynamics were theorized by the River Continuum Concept (RCC) (Vannote *et al.*, 1980). According to this model, DOM heterogeneity and processing is expected to decrease from upstream to downstream, whereas the contribution of recalcitrant molecules is expected to increase (Fellman *et al.*, 2014). Thus, larger and more reactive molecules would be more abundant in headwaters while smaller and more recalcitrant molecules would be more plentiful downriver (Amon & Benner, 1996). More recently, Creed *et al.* (2015) suggested a tendency towards a convergence/confluence of DOM concentration and composition along the river continuum. According to Creed's approach, high DOM variability and low DOM reactivity is expected in headwaters. In contrast, low DOM variability is expected downriver.

However, these scenarios ignore the impact of a succession of inputs from natural and anthropogenic tributaries (Fisher *et al.*, 2004) and the occurrence of extreme hydrological episodes (Butturini *et al.*, 2016). For instance, low in-stream DOM processing may be expected during floods due to low water residence times (Raymond *et al.*, 2016). Therefore, terrestrially-derived molecules may reach lowland river sites. During drought, long water residence times may stimulate in-stream microbial respiration (Maranger *et al.*, 2005), photochemical oxidation (Gao & Zepp, 1998) and primary production (Findlay & Sinsabaugh, 2003), thus increasing the amount of potentially labile compounds.

Predictions formulated by the RCC and successive extension and/or readjustments (Junk *et al.*, 1989; Creed *et al.*, 2015; Raymond *et al.*, 2016) motivated the study of DOM longitudinal transport and fate along fluvial networks (Fell-

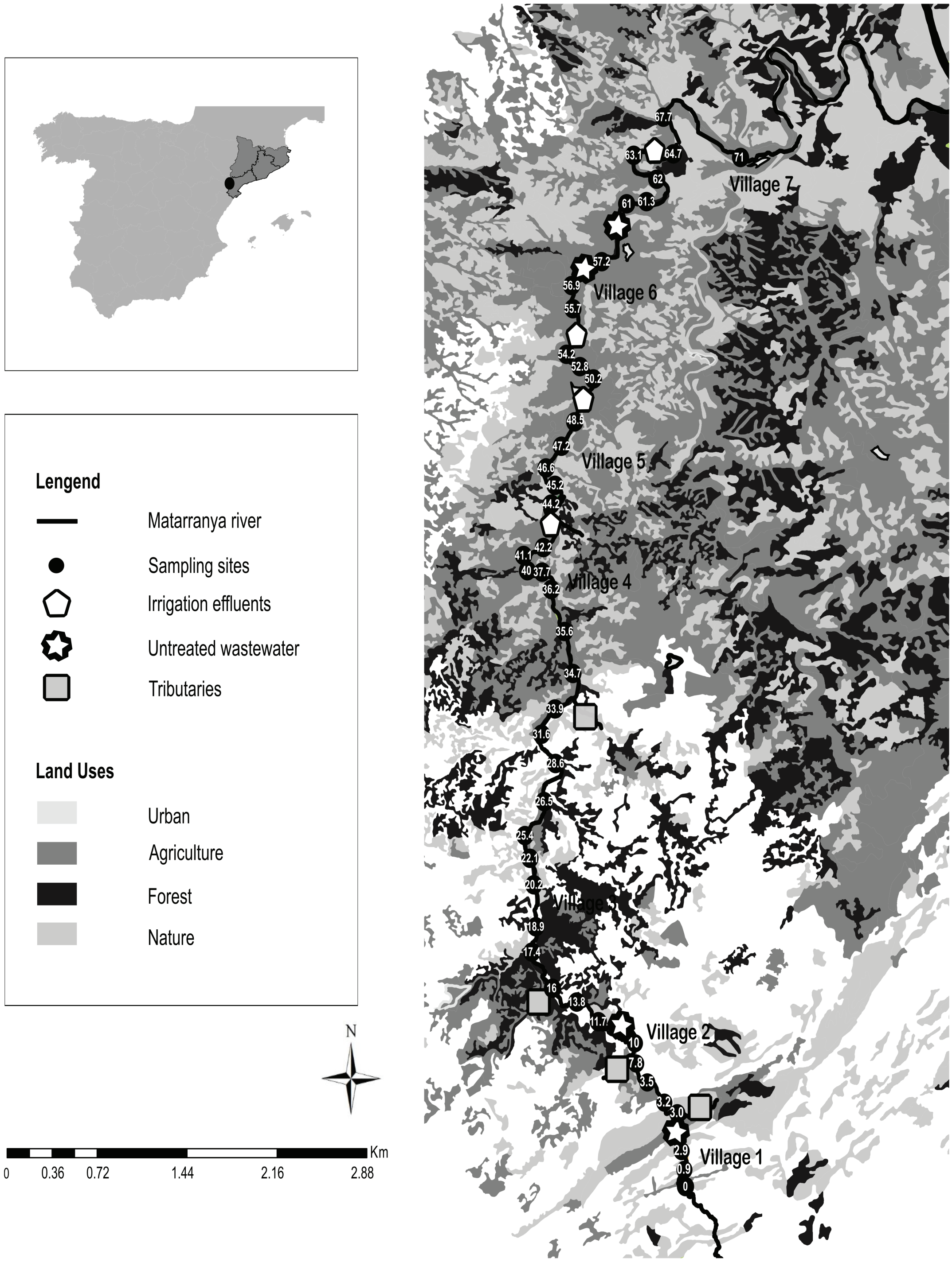

Figure 1. Matarranya river main stem and land uses. Black dots are sampling sites (numbers inside black dots indicate the distance in km from headwaters). Villages along the river are named with numbers (from 1 to 7). The villages are, beginning from the headwaters: Beseit, Vall-de-roures, La Torre del Comte, Massalió, Maella, Favara and Nonasp. *Eje principal del río Matarranya y usos del suelo. Los puntos de muestreo están indicados con círculos negros (los números en el interior de los círculos negros, muestran la distancia en km desde la cabecera). Los pueblos que se encuentran a lo largo del río, están indicados con números (del 1 al 7). Los pueblos son, desde la cabecera: Beseit, Vall-de-roures, La Torre del Comte, Massalió, Maella, Favara and Nonasp.*

man *et al.*, 2014; Kaushal *et al.*, 2014; Creed *et al.*, 2015; Wollheim *et al.*, 2015; Butturini *et al.*, 2016). Most of these studies were performed under baseflow conditions, whereas few studies have focused on drought and floods (Butturini *et al.*, 2016; Ejarque *et al.*, 2017). However, data obtained under droughts and floods are essential to understand the biogeochemical functioning of fluvial ecosystems. This is especially crucial in Mediterranean systems because a change in the frequency and magnitude of both hydrological extremes is expected in Mediterranean catchments (Vicente-Serrano *et al.*, 2014; Barrera-Escoda & Llasat, 2015).

In this context, we aimed to analyse the quantitative and qualitative changes in DOM along a longitudinal continuum of an intermittent Mediterranean river, under two contrasting hydrological conditions: drought and high flows. Our two research questions were: i) How do flow extremes determine DOM properties? ii) How does the river continuum modulate the impact of hydrology on DOM properties? According to Creed's hypothesis, we expected a reduction in the contribution of aromatic substances and concurrent increases in small and aliphatic molecules downriver. In parallel, differences in DOM quantity and quality between high and low flow conditions were expected to become smaller along the fluvial continuum. To achieve our aims, the main stem of a large intermittent river (70 km long) was sampled at high spatial frequency. DOM characterization included its quantification in terms of carbon (DOC) and qualitative DOM descriptors through spectroscopy techniques. Euclidean distance was also estimated to quantify the impact of hydrological conditions on DOM longitudinal patterns.

MATERIAL AND METHODS

Study area

This study was performed along the Matarranya river, the last important tributary joining the Ebro from the right-hand side of the river. It drains a catchment of 1738.45 km^2 from Els Ports de Tortosa-Beseit (1296 m a.s.l.) to the Ribarroja reservoir 100 km downstream (70 m a.s.l.). The basin is part of the geological Maestrazgo–Catalànides domain, which can be divided into two main areas: 1) Els Ports de Beseit, dominated by Mesozoic materials, in the headwaters; 2) The Ebro depression, dominated by Cenozoic (Tertiary and Quaternary) materials, in the middle and final sections of the Matarranya river. The geology is dominated by rocks of terrigenous origin (conglomerates, sandstones and marls), but limestones and evaporites (gypsum) outcrop along the entire route of the riverbed. The catchment is covered by brushwood (33 %), forest (14 %), urban areas (14 %) and agriculture (33 %), the latter especially in the middle and downriver reaches. The climate is relatively warm and arid. Downriver, air temperature and annual rainfall average 14-16 ºC and 350 mm respectively. In contrast, in the headwaters air temperature and annual rainfall average 12-14 ºC and 700-900 mm (El plan hidrológico del río Matarraña, 2008). The river shows a typical Mediterranean hydrology, characterized by moderate-high flow conditions in spring and autumn and a severe dry period in summer. The fluvial network contributes 156 hm^3 to the Ebro discharge. It comprises four main headwater tributaries (Matarranya, Ulldemó, Pena and Tastavins). Downriver the largest tributary is the Algars river. Fluvial hydrology is altered by human activities. There are two main reservoirs: the Pena reservoir (17 hm^3) and Vallcomuna (2.42 hm^3) as well as numerous small reservoirs in the catchment. Finally, a dense drainage system takes water from the river to irrigation systems during spring and summer. Since 1995, water from the Matarranya has been diverted into the Pena reservoir in winter (El plan hidrológico del río Matarraña, 2008). There are seven villages along the river. In the text they are named from "1" (headwaters) to "7" (downriver). The full names of the villages are given in the caption of Figure 1.

Sampling strategy

The Matarranya river was sampled along its main stem and at the main natural and anthropogenic inflows to the main stem (Fig. 1). The main stem was sampled at 45 sites, from the headwaters (2 km from source; 40° 48' 57.87" N / 0° 11' 11.94"

E) to its mouth (71 km from source; 41° 12' 40.13" N / 0° 14' 57.74" E). The surface water was sampled in the middle of the river channel. The distance between sampling sites averaged 1.6 ± 0.9 km. Sampling sites were selected in order to take into account all main tributaries (at kilometres 3, 7.5, 14, 29), untreated wastewater inputs (at kilometres 2.5, 8.5, 46, 55.6) and irrigation return waters (at kilometres 38, 40, 48.8 and 62). Samples were collected during two opposite contrasting hydrological conditions. The first set of samples was collected in July 2015, under summer drought conditions. The second set was collected under high flow conditions in November 2015, after a severe high flood event.

Chemical and field measurements

Field measurements

Electrical conductivity (EC, WTW 3310 set 1 conduct-meter) and water temperature were measured at each site. At the end of each sampling day, when samples were at the same temperature, DOM fluorescence in unfiltered samples was measured using two fluorescence sensors: a humic-like sensor (TurnerDesigns Cyclops 7, Ex/Em, 325/470nm) and a tryptophan-like sensor (TurnerDesigns Cyclops 7, Ex/Em, 285/350nm).

Chemical analyses

For chemical analyses, all samples were filtered in the field using precombusted (450 ºC) glass fibre filters (Whatman GF/F 0.7 µm pore size) and then 0.22 µm pore nylon filters. The filtered samples were placed in amber glass bottles previously washed with acid. We stored the samples on ice and in the dark, and immediately transported them to the laboratory where they were stored at 4 ºC for later analysis. Chemical parameters were grouped as follows: inorganic solutes (named DIM) included: electrical conductivity, chloride, sulphate, $^{18}\Delta O$, ΔD, ammonium (NH_4^+), nitrate (NO_3^-) and phosphate (PO_4^{3-}); DOM descriptors (named DOM) included: DOC, HIX, FI, BIX, Sr, E2:E3, $SUVA_{254}$, $SUVA_{350}$, $Fluor_{Humic\text{-}like}$ and $Fluor_{Prot\text{-}like}$.

Inorganic solutes

Ammonium concentration was measured using the salicylate method (Reardon, 1969), and the soluble reactive phosphor (SRP) was measured using the molybdate method (Murphy & Riley, 1962). Inorganic anions (nitrate, chloride and sulphate) concentrations were analysed with an ion chromatograph Metrohm 761 Compact IC with the column Metrosep A Supp5 - 150/4.0.

To perform a better geochemical discrimination between the two opposite hydrological conditions stable water isotopes $^{18}\Delta O$ and ΔD were analysed (Laudon & Slaymaker, 1997). Stable isotopes analysis were performed at the Scientific and Technological Centre of the University of Barcelona. For $^{18}\Delta O$ the equilibrium was achieved with CO_2 and He and measurements were executed on a MAT 253 from Thermofisher. ΔD was measured by water pyrolysis analysis of the resulting H_2 separated by column chromatography on an EA-TC-IRMS-DELTA PLUS xp Thermofisher.

DOC concentration and optical properties of DOM

Samples for DOC analysis only were filtered by glass fiber filters (Whatman GF/F 0.7 µm pore size) and later, they were acidified with 10 % HCl and refrigerated before analysis. DOC was determined by oxidative combustion and infrared analysis using a Shimadzu TOC Analyser VCSH coupled with a TN analyser unit. Qualitative optical properties of DOM were estimated in terms of absorbance and fluorescence. DOM absorbance spectra were measured using a UV-Visible spectrophotometer UV1700 Pharma Spec (Shimadzu) and a 1 cm quartz cell. Absorbance data were obtained in double beam mode with wavelength scanned from 200 to 800 nm and deionized water as the blank. Excitation-Emission Matrices (EEM) were generated by an RF-5301 PC spectrofluorimeter (Shimadzu). Spectra were measured using a 1 cm quartz cell. EMMs were measured over (Ex/Em) wavelengths of 240-420 nm and 280-690 nm and they were standardized based on the method of Goletz *et al.* (2011) using Mathematica (Wolfram

Research) software. EEM data were corrected using the same method. The absorbance data for each sample respectively were used to correct the inner filter effects (Lakowicz, 2006). To correct wavelength-dependent inefficiencies of the detection system the following methods were used: Gardecki & Maroncelli's method (1998) for emission measurements and Lakowicz's method (2006) for excitation correction. Data were normalized with daily measurements of the area under the Raman peak using MilliQ water blanks (Lawaetz & Stedmon, 2009).

Seven qualitative descriptors of DOM were estimated in this study The four chromophoric indices were as follows: (a) Specific Ultra Violet Absorbance at 254 nm ($SUVA_{254}$) and (b) Specific Ultraviolet Absorbance at 350 nm ($SUVA_{350}$) as the absorption coefficient at 254 or 350 nm normalized by DOC concentration (Weishaar *et al.*, 2003). Higher values are typically related to greater aromaticity (Hansen *et al.*, 2016). (c) The ratio of absorbance at 250 nm to 365 nm (E2:E3), which provides information about DOM molecular size. Low E2:E3 values suggest a proportional increase in average DOM size (De Haan & De Boer, 1987). (d) Spectral slopes ratio (S_R), which also integrates shifts in the molecular size of DOM. This is a dimensionless parameter, estimated by calculating the ratio of the logarithmically transformed absorbance spectra slope at 275–295 nm (S275–295) to that estimated at 350–400 nm (S350–400). High S_R values indicate an increase in the proportion of the small DOM molecular fraction (Helms *et al.*, 2008). Three fluorophoric indices were also estimated: (a) Humification index (HIX), which is the area under the emission spectra 435-480 nm divided by the peak area 310-345 nm from the spectra at an excitation wavelength of 254 nm. HIX indicates the extent of humification by quantifying the shift in the emission spectra toward longer wavelengths, due to lower H:C ratios. HIX values range from 0 to 1 with higher values indicating a greater degree of DOM humification (modified from Ohno, 2002). (b) Fluorescence index (FI), which is the ratio of emission intensities at 470 nm and 520 nm emitted at an excitation of 370 nm and provides information about DOM sources. High values suggest the prevalence of autochthonous DOM and low values the prevalence of allochthonous DOM (Cory & McKnight, 2005). (c) Biological index (BIX), which was calculated at an excitation of 310 nm as the ratio of the fluorescence intensity emitted at 380 nm. β fluorophore is the maximum of intensity and emitted at 430 nm, which corresponds with humic fraction. The *β* fluorophore is typical of recent autochthonous DOM release. Therefore, high BIX values (> 1) suggest the presence of autochthonous and fresh DOM, whereas BIX values of 0.6–0.7 indicate low or zero autochthonous DOM production (Huguet *et al.*, 2009).

Hydrological measurements

During drought conditions, discharge was calculated at 19 sampling sites along the main reach. The velocity-area method (Di Baldassarre & Montanari, 2009) was used. A flowmeter (Global Water FP111 Flow, sensor range 0.1-6.1 m/s) was used to measure the mean water velocity. The river channel cross-section was divided into 0.2-0.5 m subsections (depending on the river width). The mean water velocity was estimated at 2/3 of the total depth. During high flow conditions, it was not feasible to estimate discharge in situ. Discharge values from the *Confederación hidrográfica del Ebro* were available for one headwaters site (40° 49' 27.82" N; 0° 11' 7.61" E) and one downstream site (41° 11' 42.42" N; 0° 10' 17.92" E). Values at these two sites were used to interpolate discharge along the entire longitudinal continuum.

Statistical analyses

The non-parametric Mann-Whitney-Wilcoxon test (Wilcoxon, 1945; Mann & Whitney, 1947) was used to test differences in the solute content between drought and high flow conditions. Correlations between variables were considered significant at the 5 % level. Spatial and contrasting hydrological conditions (high flow and drought) variability were explored using principal components analysis (PCA). Two PCAs were run: the first one included only the DIM solutes (PCA_{DIM}). The second PCA integrated

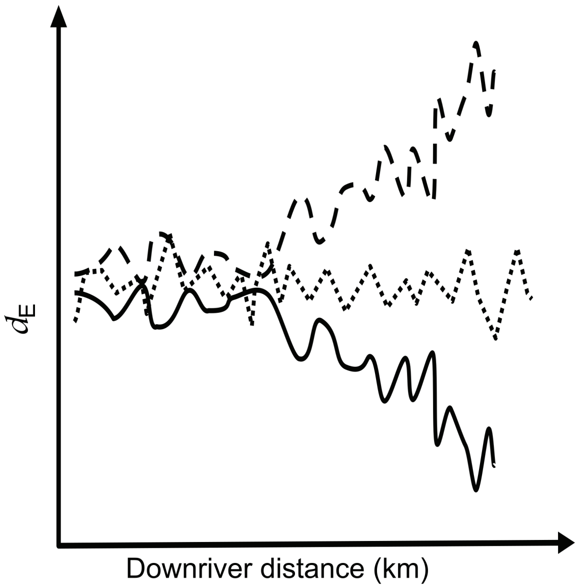

Figure 2. Three hypothetical trends in the dissimilarity index d_E with respect to the downriver distance. The dotted line describes the tendency when d_E is unrelated to the downriver distance. The dashed line describes the tendency when d_E increases downriver. The solid line describes the opposite situation, when d_E decreases downriver. Additional details are given in the statistical analyses section. *Tres tendencias hipotéticas del índice de disimilitud* d_E *respecto a la distancia aguas abajo. La línea de puntos describe la tendencia cuando* d_E *no está relacionada con la distancia aguas abajo. La línea discontinua muestra la tendencia cuando* d_E *aumenta río abajo. La línea continua describe la situación opuesta, cuando* d_E *disminuye aguas abajo. Para detalles adicionales, se encuentran en la sección de análisis estadísticos.*

ten DOM descriptors (PCA_{DOM}). Clusters in the PCA analysis were identified using the optimization significant test silhouette (Rousseeuw, 1987). In order to quantify how alterations in DOM and DIM properties, induced by hydrology, changed downriver, we estimated the Euclidean distance (d_E, thereafter) between scores obtained under drought and high flow conditions at each sampling site, and plotted these distances with respect to the downriver distance. The Euclidean distance, d_E, describes the biogeochemical dissimilarity among samples collected at the same site but under the two contrasting hydrological conditions. Low d_E values indicate low biogeochemical dissimilarity (or high similarity) among hydrological conditions i.e. high

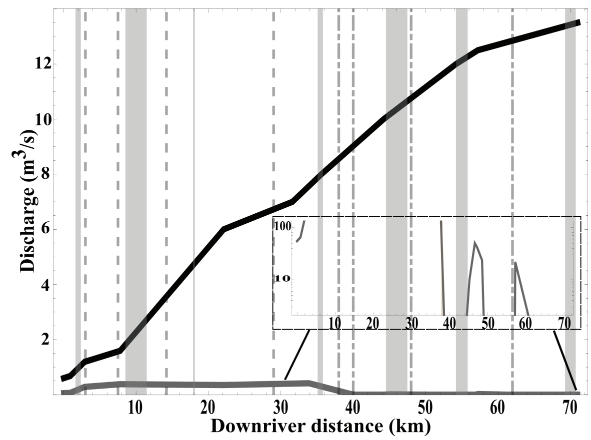

Figure 3. Longitudinal discharge profile along the river continuum during drought (horizontal grey line) and high flow (horizontal thin black line) conditions. Continuous vertical lines show the location of the seven villages next to the Matarranya river. The thickness of the lines is proportional to population size. Dashed vertical lines on the left show the location of the main affluent. Dashed vertical lines on the right are the irrigation return flows. The inset shows the discharge at most downriver sites during drought. Discharge under high flow conditions (thin black line) was interpreted for illustrative purpose only, because discharge was only available for kilometre 0.9 and 58. Discharges were interpolated assuming that the discharge increased downriver according to a potential model. *Perfil longitudinal del caudal a lo largo del continuo fluvial en condiciones de sequía (línea gris horizontal) y caudal alto (línea negra horizontal). Las líneas verticales continuas muestran la localización de los pueblos de alrededor del río Matarranya. El grosor de las líneas es proporcional al tamaño de la población. Las líneas discontinuas verticales de la izquierda, indican la localización de los afluentes principales. Las líneas discontinuas verticales de la derecha, indican la ubicación de los puntos de extracción de agua para el regadío. El recuadro muestra el caudal durante el periodo de sequía en la mayoría de puntos de muestreo aguas abajo. El caudal en condiciones de flujo alto (línea negra delgada) ha sido interpretado con una finalidad ilustrativa debido a que este solo está disponible del kilómetro 0.9 a 58. Los caudales fueron interpolados asumiendo que estos se incrementaron aguas abajo, se ha desarrollado a partir de un modelo potencial.*

chemostasis. High d_E values indicate the opposite (Fig. 2). Two dissimilarity indices were estimated: one for inorganic solutes ($d_{E\text{-}DIM}$) and the other for DOM ($d_{E\text{-}DOM}$) parameters. Normality was tested using the Kolmogorov–Smirnov test (Massey, 1951). The null hypothesis was rejected at 5 %. Mathematica (Wolfram Research) software was used for all statistical analyses.

RESULTS

Hydrology

Under drought conditions, discharge increased gradually from 0.055 to 0.55 m^3/s from the source to kilometre 12 (just after village 2). It then decreased to 0.4 m^3/s at kilometre 35. From this site, all water was taken for irrigation and runoff was nil, except in villages 5 and 6. From kilometre 40 to the last sampling site (kilometre 71) the fluvial continuum vanished, and water was confined to isolated and stagnant pools. The discharge profile was clearly different under high flow conditions. According to the information provided by the *Confederación hidrográfica del Ebro*, discharge increased from 0.61 m^3/s between the source and kilometre 58 to 12.5 m^3/s at the final downriver site (kilometre 71) (Fig. 3).

Inorganic solute concentrations. Drought vs. high flow

Under drought conditions, EC values ranged from 473 (headwaters) to 2060 µS/cm (kilometre 47) and were significantly higher than during high flow (U = 1597, $p < 0.001$; Fig. 4a). The highest increases started at kilometre 40 and

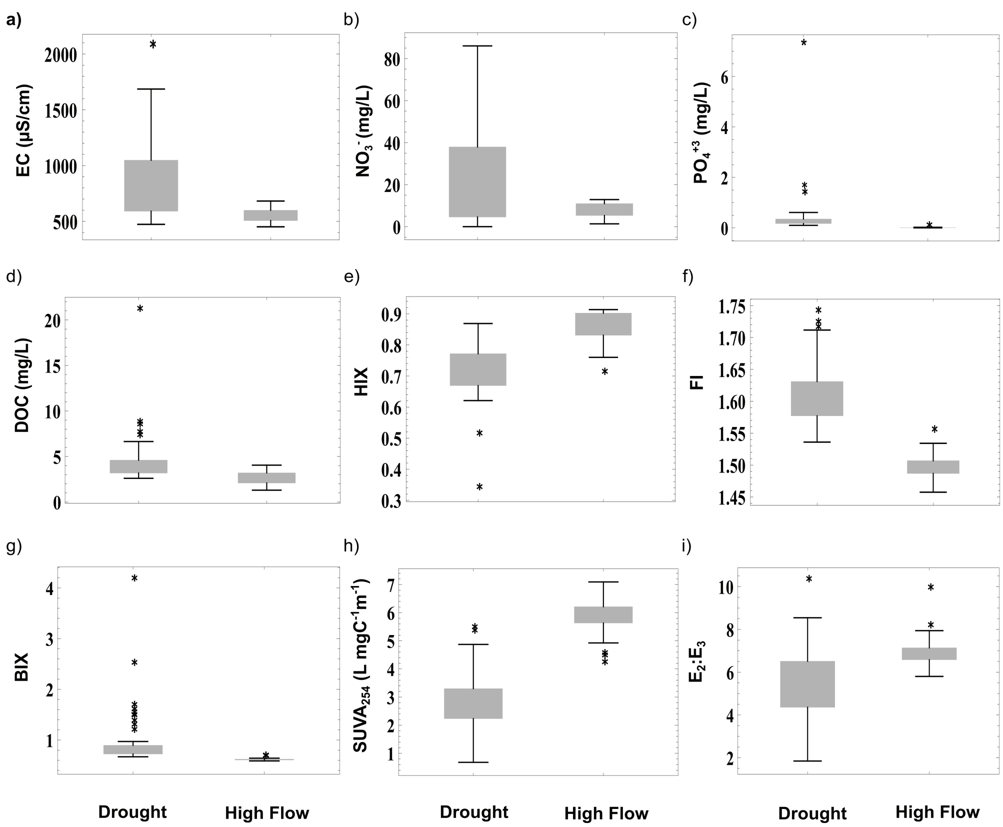

Figure 4. Box plots summarize the differences between drought (left box plot) and high flow (right box plot) conditions for the following variables: a) electrical conductivity (EC), b) nitrate (NO_3^-), c) phosphate ($PO4^{3+}$), d) dissolved organic carbon (DOC), e) humification index (HIX), f) fluorescence index (FI), g) biological index (BIX), h) specific ultra-violet absorbance at 254 nm ($SUVA_{254}$) and i) ratio of absorbance at wavelength 250nm:365nm (E_2:E_3). Asterisks symbolized the outliers of each variable. *Los diagramas de caja resumen las diferencia entre condiciones de sequía (diagrama de caja de la izquierda) y caudal alto (diagrama de caja de la derecha) para las siguientes variables: a) conductividad eléctrica (EC), b) nitrato (NO_3^-), c) fosfato ($PO4^{3+}$), d) carbono orgánico disuelto (DOC), e) índice de humificación (HIX), f) índice de fluorescencia (FI), g) índice biológico (BIX), h) absorbancia específica ultra-violeta a 254 nm ($SUVA_{254}$) y i) ratio de absorbancia en una longitud de onda de 250nm:365nm (E_2:E_3). Los asteriscos indican valores atípicos de cada variable.*

peaks occurred at kilometres 47, 56 and 62 (corresponding to wastewater effluents from villages 5, 6, and irrigation return flows, respectively) (Fig. 5a). During high flow, conductivity increased slightly along the fluvial continuum from 451 (headwater) to 671 μS/cm (downriver). Abrupt increases were minor and occurred at kilometre 15 (after the confluence with the Tastavins affluent) and at kilometre 56 (village 6). Nitrate (NO_3^-) concentrations were significantly higher during drought conditions than during high flows (U = 1485, $p < 0.001$; Fig. 4b) with values oscillating from 0.59 to 86 mg/L. Lower concentrations were typically found in the headwaters, but the concentration increased abruptly to 32 mg/L at kilometre 18 (village 3) (Fig. 5b). Downstream, the NO_3^- concentration remain relatively stable until kilometre 45 and additional abrupt increases were detected downstream from the untreated wastewater inputs at village 5 (kilometre 47, 86.01 mg/L) and 6 (kilometre 57, 70.10 mg/L). Under high flows, the NO_3^- concentration increased from 1.34 (headwaters) to 12 mg/L (kilometre 57) then decreased to less than 2 mg/L up to kilometre 71. Phosphate (PO_4^{-3}) concentrations were significantly higher during drought (U = 2025, $p < 0.001$; Fig. 4c). PO_4^{-3} concentrations ranged between 0.10 and 7.13 mg/L during drought (Fig. 5c). The highest concentrations were recorded at kilometres 10, 47 and 56 just downstream from the untreated wastewaters at villages 2, 5 and 6, respectively. During high flow, phosphate concentrations were typically lower than the detection level (< 0.005 mg/L) in headwaters and around 0.03 mg/L at downstream sites.

DOM concentrations and properties. Drought vs. high flow

DOM was significantly higher under drought conditions than during high flow (in terms of DOC concentration, U = 1747, $p < 0.001$, Fig. 4d). It was also less humified (in terms of HIX, U = 150, $p < 0.001$; Fig. 4e), less aromatic (in terms of $SUVA_{254}$, U = 18, $p < 0.001$; Fig. 4h), more autochthonous (in terms of FI, U = 2022, $p < 0.001$; Fig. 4f), more fresh (in terms of BIX, U = 20225, $p < 0.001$; Fig. 4g) and smaller in size (in terms of E2:E3, U = 284, $p < 0.05$, Fig. 4i). DOC concentrations ranged between 2.60 and 21.05 mg/L during drought conditions, with no clear longitudinal trend (Fig. 5d). However, the largest abrupt concentration increases coincided with untreated wastewater inputs (kilometres 10, 47 and 56) and an irrigation return flow (kilometre 49). Under high flow, DOC concentrations increased progressively downriver from 1.30 (kilometre 0.1) to 4.05 mg/L (kilometre 71). HIX values ranged between 0.34 and 0.87 during drought. The lowest values were found between kilometres 12 (village 2) and 17 (village 3) (Fig. 5e). Downriver from these sites, the HIX values gradually increased up to 0.85. Under high flow, HIX values ranged between 0.76 and 0.91. The lowest values were detected in the headwaters (from kilometre 0 to 14). Thereafter they remained relatively constant at around 0.9. FI fluctuated between 1.54 and 1.74 and tended to decrease along the river continuum during drought (Fig. 5f). The highest values were detected at kilometre 0.9 (headwater) and 10, 47 and 56 (coinciding with untreated wastewater inputs). On the other hand, FI did not show any longitudinal trend under high flow conditions. Peak FI values coincided with villages 1, 2, 3, 5 and 6. Under drought conditions, the highest BIX value was detected at kilometre 10 (coinciding with wastewater input from village 2, Fig. 5g). Downstream, the BIX value decreased rapidly to less than 1. However, two additional peaks were detected at kilometres 17 and 26. During high flow, BIX values fluctuated between 0.56 and 0.66 along the main stem and did not show any longitudinal trend. $SUVA_{254}$ showed a tendency to increase downriver during both hydrological conditions. In contrast to other DOM descriptors, residual waters did not show any consistent change in $SUVA_{254}$. For instance, this index was slightly lower (or unchanged) at villages 2, 3 and 5, and only increased after village 6 during drought conditions (Fig. 5h). The spectral slope index (Sr) showed larger fluctuations and a longitudinal pattern during drought conditions than during high flow although the differences in Sr values between the two hydrological periods were not statistically significant (U = 1176, n.s.). Higher Sr values were detected in headwaters

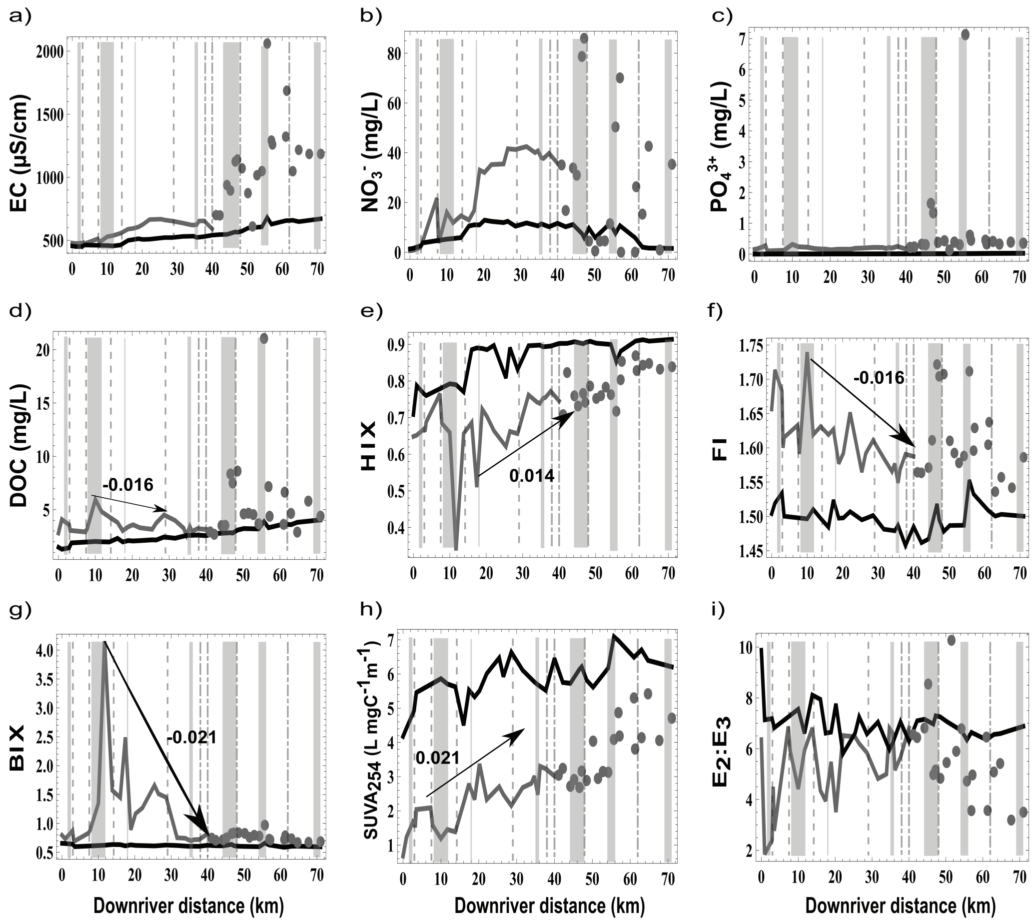

Figure 5. Longitudinal profiles, along the river continuum, of the same variables detailed in figure 4 during drought (horizontal grey line and grey dots) and high flow (horizontal black line) conditions. Grey dots remark that, from kilometer 40 the water samples were collected from isolated pools. Vertical lines are the same as those in figure 3. Arrows emphasize the longitudinal linear trend of some DOM parameters from kilometres 10 to 45. The values show the rescaled slope of these trends (statistical significance of all slopes are of $p < 0.01$). See discussion for additional information. *Perfiles longitudinales a lo largo del continuo fluvial, con las mismas variables detalladas en la figura 4 durante condiciones de sequía (línea gris horizontal y círculos grises) y condiciones de caudal alto (línea negra horizontal). Los círculos grises indican que a partir del kilómetro 40, las muestras de agua se han obtenido de las balsas aisladas. Líneas verticales son las mismas que en la figura 3. Las flechas enfatizan la tendencia lineal de algunos parámetros de la MOD desde el kilómetro 10 al 45. Los valores muestran la tendencia de las pendientes reescaladas (diferencias significativas de todas las pendientes con* p *< 0.01). Información adicional en la discusión.*

under drought conditions. Downstream Sr decreased rapidly until kilometre 27 and then gradually increased up to kilometre 68. On the other hand, the Sr values decreased slightly from 1.1 to 0.9 during high flow conditions. Under drought conditions the E_2:E_3 ratio showed marked oscillation between 2 and 10, with a minimum at kilometre 0.9 and a maximum at kilometre 52 (Fig. 5i). Under high flow E_2:E_3 was relatively steady between 5 and 8 along the longitudinal axis, with the highest value at the headwater site (E_2:E_3~10).

Principal component analysis and $d_{E\text{-}DIM}$ and $d_{E\text{-}DOM}$ along the fluvial continuum

Figure 6 shows the scores of the first and second components obtained from the PCA_{DIM} (the inorganic solutes). The two main components explained 59 and 18 % of the total variance

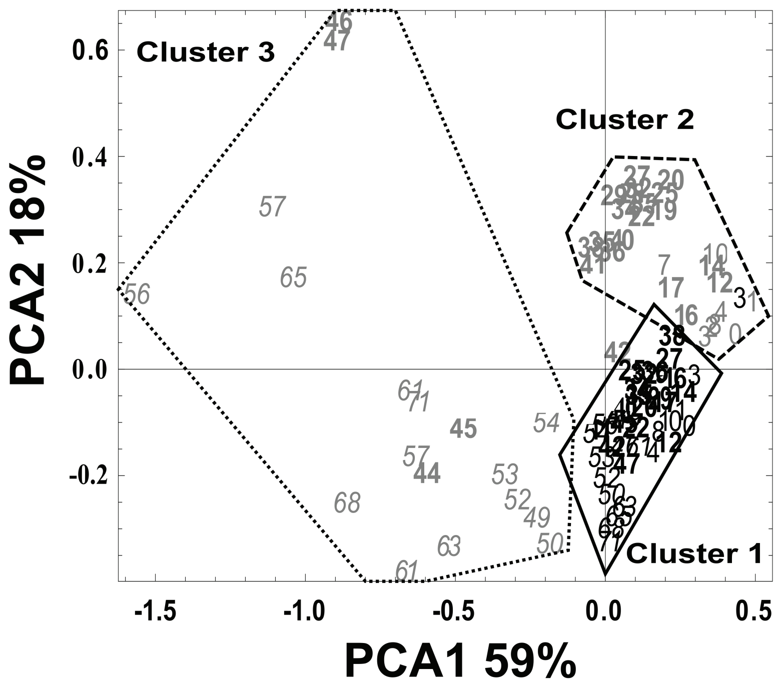

Figure 6. Principal component analysis of the inorganic solutes (PCA_{DIM}). Variables are: electrical conductivity, chloride, sulphate, $^{18}\Delta O$, ΔD, ammonium, nitrate and phosphate. Grey values are samples collected under drought conditions. Black values are samples collected under high flow conditions. Values indicate the distance (in kilometres) from the headwaters. Normal font show headwaters sites from 0 to 10 km. Bold font show middle channel sites from 11 to 47 km. Italic font show downstream sites from 48 to 71 km. Clusters were obtained using the Silhouette significance test. *Análisis de componente principal de solutos inorgánicos (PCA_{DIM}). Las variables son: conductividad eléctrica, cloruro, sulfato, $^{18}\Delta O$, ΔD, amonio, nitrato y fosfato. Valores en gris indican el resultado en condiciones de sequía y en negro, condiciones de caudal alto. Los números indican la distancia (en kilómetros) desde la cabecera del río. La fuente normal presenta los puntos de muestreo situados en la cabecera, desde 0 a 10 km. En negrita, muestra los ubicados en el cauce medio desde los 11 kilómetros a los 47. En cursiva, los puntos de muestreo aguas abajo desde los 48 kilómetros a los 71. Los grupos fueron obtenidos a partir de la prueba de significancia de silueta.*

respectively. PCA1 separated the data, under drought conditions, according to their location. Silhouette analysis identified three main clusters: Cluster #1 (negative PCA2 scores) integrated all data collected during high flow conditions. Cluster #2 (positive PCA2 scores) integrated data from headwaters and middle reaches (up to kilometre 45) under drought conditions. Cluster #3 (negative PCA1 scores) was the most heterogeneous and integrated mainly data from downstream sampling sites (from kilometre 46 to kilometre 71) under drought conditions.

PCA of the DOM parameters explained 78 % of total data set variance (Fig. 7). PCA1 axis (59 % of total variance), separated the data set according to hydrology. High flow conditions were associated with negative PCA1 scores and drought conditions with positive PCA1 scores. The inset in figure 7 shows that PC1 scores decreased from nil to more negative values from headwaters to middle reaches and downstream reaches. PCA2 explained 19 % of the total variance. This axis separated the data collected under drought conditions according to their location along the main stem: headwaters and middle reaches with positive scores and downstream with negative scores. Data separation along the fluvial continuum was much more gradual during high flow conditions. Silhouette analysis revealed two clusters: Cluster #1 integrated samples collected from headwaters and middle reaches during the drought episode. Cluster #2 integrated samples collected during high flow and most of the downstream samples collected during drought.

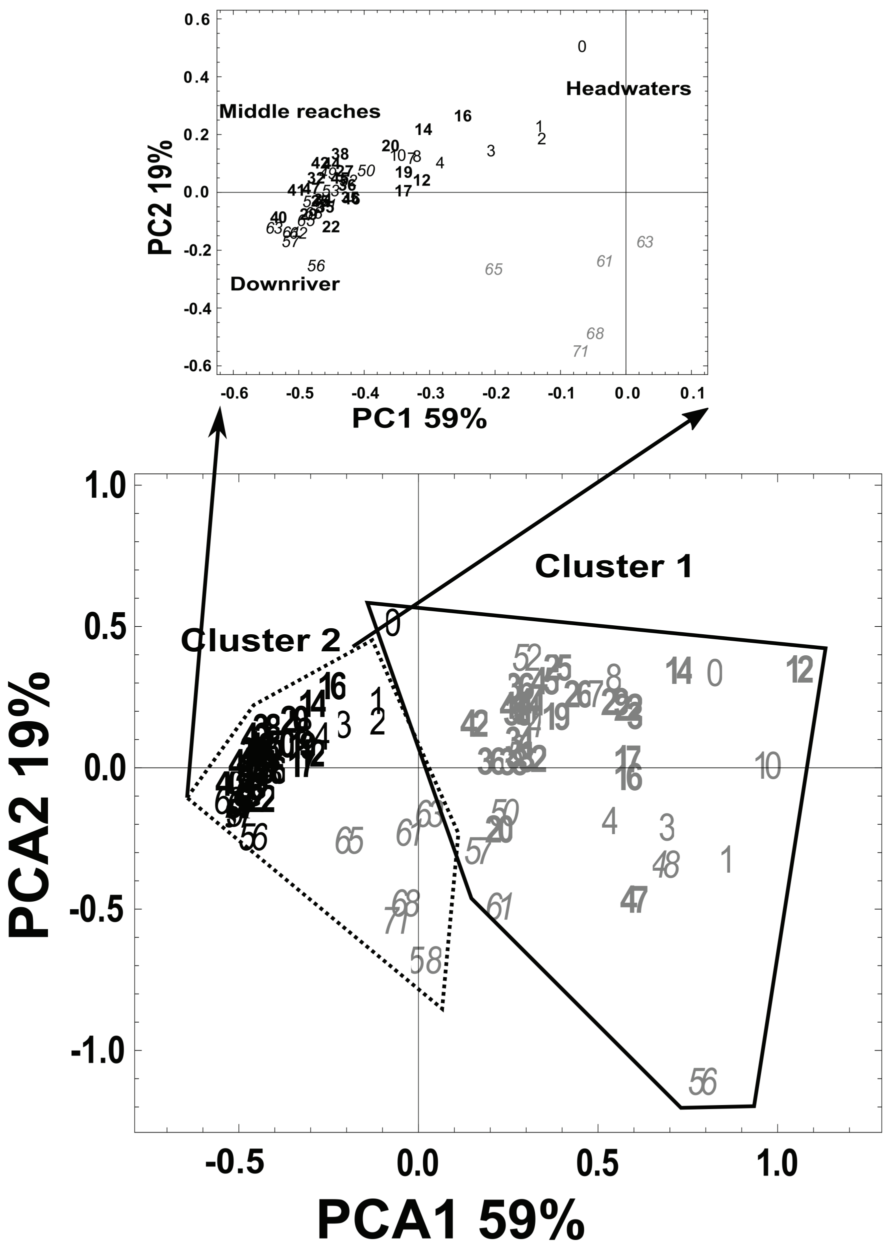

Figure 7. Principal component analysis of the dissolved organic matter parameters. Variables are: DOC, HIX, FI, BIX, Sr, E2:E3, $SUVA_{254}$, $SUVA_{350}$, $Fluor_{Humic\text{-}like}$ (FlHu) and $Fluor_{Prot\text{-}like}$ (FlPr). Grey values are samples collected under drought conditions. Black values are samples collected under high flow conditions. Values indicate the distance (in kilometres) from the headwaters. Normal font show headwaters sites from 0 to 10 km. Bold font show middle channel sites from 11 to 47 km. Italic font show downstream sites from 48 to 71 km. Clusters were obtained using the Silhouette significance test. The inset expands the PCA plot for data collected during high flow conditions. *Análisis de componente principal de los parámetros de la materia orgánica disuelta. Las variables son: DOC, HIX, FI, BIX, Sr, E2:E3, $SUVA_{254}$, $SUVA_{350}$, $Fluor_{Humic\text{-}like}$ (FlHu) and $Fluor_{Prot\text{-}like}$ (FlPr). Valores en gris indican el resultado en condiciones de sequía y en negro, condiciones de caudal alto. Los números indican la distancia (en kilómetros) desde la cabecera del río. La fuente normal presenta los puntos de muestreo situados en la cabecera, desde 0 a 10 km. En negrita, muestra los ubicados en el cauce medio desde los 11 kilómetros a los 47. En cursiva, los puntos de muestreo aguas abajo desde los 48 kilómetros a los 71. Los grupos fueron obtenidos a partir de la prueba de significancia de silueta. El recuadro amplía el gráfico de la PCA para los datos obtenidos en caudal alto.*

Figure 7 presents the longitudinal trend of the dissimilarity indices obtained for the DIM and DOM parameters (d_{E}-DIM and $d_{E\text{-}DOM}$ respectively) along the main stem of Matarranya river. A gradual and significant decrease in $d_{E\text{-}DOM}$ was detected along the river continuum ($r^2 = 0.1$, d.f. = 43, $p < 0.05$). This trend suggests that the qualitative properties of DOM tended to be unrelated to hydrological oscillations at the downriver sites. The trend is even more significant if the abrupt increase in dissimilarity that emerged downstream from the untreated wastewater inputs at village 2 (kilometre 10), village 5 (kilometre 46) and village 6 (kilometre 55) is removed ($r^2 = 0.45$, d.f. = 43, $p < 0.001$). On the other hand, the dissimilarity index of inorganic solutes (dE-DIM) showed the opposite trend to the DOM trend and increased significantly downriver ($r^2 = 0.32$, d.f. = 43, $p < 0.001$). However, dE-DIM was low and relatively constant from the headwaters to kilometre 40 and the dissimilarity index increased abruptly downstream from the wastewater inputs.

DISCUSSION

This study clearly demonstrates that hydrological conditions strongly affect the concentration of inorganic solutes (DIM) and quantity and properties of organic solutes (DOM) that flow along a fluvial continuum. However, the significance of the impact depends on biogeochemistry composition (i.e. DIM or DOM) and, additionally the impact is not uniformly distributed throughout the fluvial continuum. The river continuum thus exerted some control on biogeochemical responses related to hydrological variability. This control was evident for DOM but not for DIM.

Drought vs. high flow conditions: DOM quality

DOM properties were affected by hydrological conditions as follows: DOM was fresher and less degraded (high BIX), and more aliphatic and less humified (low SUVA254 and HIX respectively) under drought conditions than under high flow conditions. This suggests that it is more autochthonous (high FI and low HIX) under drought conditions and more allochthonous (low FI and high HIX) under high flow conditions. This is consistent with other studies performed in human-altered Mediterranean rivers (Ejarque Gonzalez, 2014; Butturini *et al.*, 2016). However, some caution is necessary regarding the term "autochthonous". This term means that the DOM fraction is a byproduct of in-stream processes. However, it is well known that DOM from (treated and untreated) wastewater produces a fluorescent signal associated with small protein-like substances (Baker, 2002; Saadi *et al.*, 2006; Butturini & Ejarque, 2013). This fluorescence moiety modifies the excitation-emission florescence matrices, resulting in high FI and BIX values and low HIX values. Therefore, the high FI and BIX values detected under drought conditions do not necessarily indicate in-stream autochthonous DOM generation. On the contrary, the most relevant increases in BIX and FI were abrupt and coincided with villages 2, 5 and 6, revealing the severe impact of wastewater discharge from these villages. Therefore, it is important to take into account these anthropogenic inputs.

Overall, additional anthropogenic DOM inputs appeared to be minor between village 2 (kilometre 10) and village 5 (kilometre 45). Consequently, village 3 and 4 did not alter the DOM signal (although, nitrate increased sharply at village 4 under drought conditions). In addition, the two effluents that drain into the main stem (Tastavins and Calapatos) were almost completely dry during the summer sampling. Therefore, in this large 35-km-long fluvial segment, allochthonous (natural and anthropogenic) DOM inputs should be insignificant under drought conditions. Thus, longitudinal changes in qualitative DOM detected in this segment under drought conditions, might provide information about the magnitude of in-situ DOM processing. The results show that downriver from the suspected anthropogenic DOM inputs at village 2, DOM decreased slightly in terms of concentration (i.e. dDOC/dX = -0.016 km^{-1}) and increased in terms of aromaticity (i.e. dSUVA/dX = 0.021 km^{-1}) and humification (i.e. dHIX/dX = 0.014 km^{-1}). These findings suggest the longitudinal accumulation of aromatic and large molecules,

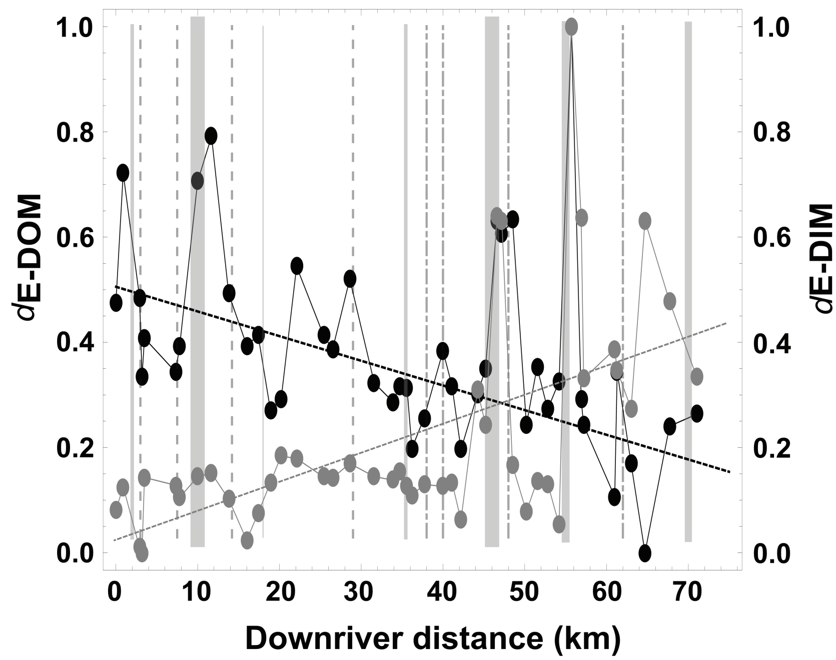

Figure 8. Longitudinal profile of the dissimilarity index of DIM ($d_{E\text{-}DiM}$, grey disks) and DOM properties ($d_{E\text{-}DOM}$, black disks) along the river continuum. Vertical lines are the same as those in figure 3. The dashed black and grey lines show the linear model ($p < 0.05$) that relates dissimilarity of the $d_{E\text{-}DOM}$ or $d_{E\text{-}DiM}$ index to the downriver distance respectively. *Perfil longitudinal del índice de disimilitud de la MID (*$d_{E\text{-}DiM}$*, discos grises) y de las propiedades de la MOD (*$d_{E\text{-}DOM}$*, discos negros) a lo largo del continuo fluvial. Las líneas verticales son las mismas que en la figura 3. Las líneas discontinuas horizontales negra y gris, indican un modelo lineal (*$p < 0.05$*) que muestra el índice de disimilitud* $d_{E\text{-}DOM}$ *o* $d_{E\text{-}DiM}$ *respecto a la distancia aguas abajo.*

probably as a consequence of the degradation of labile aliphatic substances and the concurrent accumulation of more refractory aromatic humics. The gradual decrease in the FI index (dFI/dX= -0.016 km^{-1}) and the decrease in the BIX index (dBIX/dX= -0.021 km^{-1}) also suggest the degradation of labile substances. Remarkably, $SUVA_{254}$ increased at a constant rate throughout the entire fluvial stem from kilometre 10 to 71. This increase, although less pronounced, was also significant under high flow conditions. Overall, this positive trend contrasts with that observed in la Tordera (Ejarque *et al.*, 2017) and that reported by Creed *et al.* (2015). They attributed the longitudinal decrease in aromatic substances to losses in allochthonous aromatic DOM and a parallel increase in autochthonous aliphatic DOM. Accordingly, this DOM processing route appeared to be inconsistent in the Matarranya river.

DOM dissimilarity trend along the river continuum

The dissimilarity index of the DIM pool ($d_{E\text{-}DIM}$) increased significantly downriver. However, a more detailed analysis revealed that $d_{E\text{-}DIM}$ was relatively steady, and relatively low, from kilometre 0 to 42, indicating that the chemical variability of DIM solutes related to high flow and drought conditions was unrelated to river size. The $d_{E\text{-}DIM}$ descriptor increased abruptly as a consequence of the impact of wastewater inputs at villages 5 and 6 under drought conditions, when, from kilometre 43 to 71, the river was totally dry and most of the discharge was from these anthropogenic sources. The position of these abrupt increases in $d_{E\text{-}DIM}$ (at kilometre 46 and 56 respectively) reduce the significance of the $d_{E\text{-}DIM}$ vs. downriver distance relationship. Therefore, the longitudinal increase in $d_{E\text{-}DIM}$

seems to be unrelated to river size: if wastewater inputs were located in the headwaters the observed positive longitudinal trend in $d_{\text{E-DIM}}$ would probably vanish.

In contrast, the $d_{\text{E-DOM}}$ showed a clear and robust tendency to decrease downriver. According to the results, hydrological oscillations affect the DOM composition of headwaters more severely than at downriver sites. The negative trend is robust enough to dampen the noise (i.e. abrupt high $d_{\text{E-DOM}}$ values) caused by the impact of anthropogenic wastewater inputs under drought conditions. Overall, this negative trend is consistent with the hypothesis proposed by Creed *et al.* (2015). These authors suggested that the impact of hydrological variability should decrease downriver and that a river will tend towards chemostasis. This situation is thought to reflect the hydrological, biogeochemical and biological factors that control variations in DOM quantity and quality in time and space. Accordingly, high DOM oscillations are expected in headwaters, where hydrological conditions determine the drainage of different soils and ground water sections and stimulate the leaching of allocthonous DOM. The hyporheic and riparian interfaces (Butturini *et al.*, 2003) are hydro-chemical compartments that can strength terrestrial-aquatic connections in headwaters and thus condition the mobilization and composition of DOM in these ecosystems (Vázquez *et al.*, 2007, 2015). On the other hand, the strength of these connections should decrease downriver. DOM in downriver reaches reflects the mixing of DOM inputs from allochthonous (natural and/or anthropogenic tributaries and groundwater) and autochthonous sources. In fact, low river gradients, enhanced water residence times and instream autochthonous biogeochemical processes are reported to be more relevant in downriver reaches.

CONCLUSION

This study demonstrates the drastic impact of the hydrological regime on DOM properties. More significantly, it reveals that variations in DOM are more notable in headwaters than downriver reaches. This result is consistent with the chemostatic hypothesis formulated by Creed *et al.* (2015). DOM properties drastically changed with both hydrological regimes. Terrigenous, humified, aromatic and degraded DOM is flushed downriver under high flow conditions. Furthermore, these properties gradually become more predominant downriver. In contrast, DOM is less degraded, more aliphatic and less humic under drought conditions. These properties were mainly determined by putative inputs of wastewater rather than in-stream autochthonous processes. Under drought conditions, the fluvial segment between village 2 (kilometre 10) and village 5 (kilometre 43) did not receive relevant anthropogenic inputs. Therefore, this large segment is appropriate for exploring the magnitude of in-stream DOM retention/release processes under low flow conditions. The results demonstrated a depletion of DOC and a decrease in the fresh and poorly degraded DOM pool: on the contrary, the the most aromatic and humified DOM pool accumulated significantly downriver. These findings contrast with those reported in other studies (Creed *et al.*, 2015; Ejarque *et al.*, 2017).

ACKNOWLEDGEMENTS

We would like to thank Alba Guarch, Astrid Harjung, Francesc Sabater, Eusebi Vazquez and Aida Viza, for field and laboratory assistance. We thank two anonymous reviewers for their stimulating comments that strongly helped to improve the original manuscript. This research was funded by the Spanish Ministry of Education and Science (MEC) (CGL2014-5876-C3-R) and the European Union 7th Framework Programme (No. 603629-ENV-2013-6.2.1-Globaqua). AB is a member of the research group ForeStream (2014SGR949). This work is dedicated to Dani Azpetia.

REFERENCES

AMON, R.M.W. & R. BENNER. 1996. Bacterial utilization of different size classes of dissolved organic matter. *Limnology and Oceanography*, 41 (1): 41–51. DOI: 10.4319/lo.1996.41.1.0041

BAKER, A. 2002. Fluorescence Excitation−Emission Matrix Characterization of River

Waters Impacted by a Tissue Mill Effluent. *Environmental Science & Technology*, 36 (7): 1377–1382. DOI: 10.1021/es0101328

BARRERA-ESCODA, A. & M.C. LLASAT. 2015. Evolving flood patterns in a Mediterranean region (1301–2012) and climatic factors – the case of Catalonia. *Hydrology and Earth System Science*, 19 (1): 465–483. DOI: 10.5194/hess-19-465-2015

BENNER, R. 2003. Molecular Indicators of the Bioavailability of Dissolved Organic Matter. *Aquatic Ecosystems*, 121–137.

BUFFAM, I., J.N. GALLOWAY, L.K. BLUM & K.J. MCGLATHERY. 2001. A stormflow/baseflow comparison of dissolved organic matter concentrations and bioavailability in an Appalachian stream. *Biogeochemistry*, 53 (3): 269–306. DOI: 10.1023/A:1010643432253

BUTTURINI, A., S. BERNAL, C. HELLIN, E. NIN, L. RIVERO, S. SABATER & F. SABATER. 2003. Influences of the stream groundwater hydrology on nitrate concentration in unsaturated riparian area bounded by an intermittent Mediterranean stream. *Water Resources Research*, 39: 1110. DOI: 10.1029/2001WR001260

BUTTURINI, A. & E. EJARQUE. 2013. Technical Note: Dissolved organic matter fluorescence – a finite mixture approach to deconvolve excitation-emission matrices. *Biogeosciences*, 10 (9): 5875–5887. DOI: 10.5194/bg-10-5875-2013

BUTTURINI, A., A. GUARCH, A.M. ROMANÍ, A. FREIXA, S. AMALFITANO, S. FAZI & E. EJARQUE. 2016. Hydrological conditions control in situ DOM retention and release along a Mediterranean river. *Water Research*, 99: 33–45. DOI: 10.1016/j.watres.2016.04.036

CONFEDERACIÓN HIDROGRÁFICA DEL EBRO. 2008. El plan hidrológico del río Matarraña. Versión V.1 http://contratoderiomatarranya.org/documentos/PHN_matarranya.pdf

CORY, R.M. & D.M. MCKNIGHT. 2005. Fluorescence Spectroscopy Reveals Ubiquitous Presence of Oxidized and Reduced Quinones in Dissolved Organic Matter. *Environmental Science & Technology*, 39 (21): 8142–8149. DOI: 10.1021/es0506962

CREED, I.F., D.M. MCKNIGHT, B. PELLERIN, M.B. GREEN, B. BERGAMASCHI, G.R. AIKEN, D.A. BURNS, S.E.G. FINDLAY, J.B. SHANLEY, R. STRIEGL, B.T. AULENBACH, D.W. CLOW, H. LAUDON, B.L. MCGLYNN, K.J. MCGUIRE, R.A. SMITH & S.M. STACKPOOLE. 2015. The river as a chemostat: fresh perspectives on dissolved organic matter flowing down the river continuum. *Canadian Journal of Fisheries and Aquatic Sciences*, 72 (8): 12721285. DOI: 10.1139/cjfas-2014-0400

DE HAAN, H. & T. DE BOER. 1987. Applicability of light absorbance and fluorescence as measures of concentration and molecular size of dissolved organic carbon in humic Lake Tjeukemeer. *Water Research*, 21 (6): 731–734. DOI: 10.1016/0043-1354(87)90086-8

DI BALDASSARRE, G. & A. MONTANARI. 2009. Uncertainty in river discharge observations: a quantitative analysis. *Hydrology and Earth System Science*, 13 (6): 913–921. DOI: 10.5194/hess-13-913-2009

EJARQUE GONZALEZ, E. 2014. *From flood to drought: Transport and reactivity of dissolved organic matter along a Mediterranean river*. Ph.D. Thesis. University of Barcelona, Spain. TDX (Tesis Doctorals en Xarxa).

EJARQUE, E., A. FREIXA, E. VAZQUEZ, A. GUARCH, S. AMALFITANO, S. FAZI, A.M. ROMANÍ & A. BUTTURINI. 2017. Quality and reactivity of dissolved organic matter in a Mediterranean river across hydrological and spatial gradients. *Science of The Total Environment*, 599–600: 1802–1812. DOI: 10.1016/j.scitotenv.2017.05.113

FELLMAN, J.B., E. HOOD & R.G.M. SPENCER. 2010. Fluorescence spectroscopy opens new windows into dissolved organic matter dynamics in freshwater ecosystems: A review. *Limnology and Oceanography*, 55 (6): 2452–2462. DOI: 10.4319/lo.2010.55.6.2452

FELLMAN, J.B., R.G.M. SPENCER, P.A. RAYMOND, N.E. PETTIT, G. SKRZYPEK, P.J. HERNES & P.F. GRIERSON. 2014. Dissolved organic carbon biolability decreases along with its modernization in fluvial networks in an ancient landscape. *Ecology*, 95 (9): 2622–2632. DOI: 10.1890/13-1360.1

FINDLAY, S. & R.L. SINSABAUGH. 2003. *Aquatic Ecosystems: Interactivity of Dissolved Organic Matter*. Academic Press, Elsevier Science.

FISHER, S.G., R.A. SPONSELLER & J.B. HEFFERNAN. 2004. Horizons in Stream Biogeochemistry: Flowpaths to Progress. *Ecology*, 85 (9): 2369–2379. DOI: 10.1890/03-0244

GAO, H. & R.G. ZEPP. 1998. Factors Influencing Photoreactions of Dissolved Organic Matter in a Coastal River of the Southeastern United States. *Environmental Science & Technology*, 32 (19): 2940-2946. DOI: 10.1021/es9803660

GARDECKI, J.A. & M. MARONCELLI. 1998. Set of Secondary Emission Standards for Calibration of the Spectral Responsivity in Emission Spectroscopy. *Applied Spectroscopy*, 52 (9): 1179–1189. DOI: 10.1366/0003702981945192

GOLETZ, C., M. WAGNER, A. GRÜBEL, W. SCHMIDT, N. KORF & P. WERNER. 2011. Standardization of fluorescence excitation–emission-matrices in aquatic milieu. *Talanta*, 85 (1): 650–656. DOI: 10.1016/j.talanta.2011.04.045

HANSEN, A.M., T.E.C. KRAUS, B.A. PELLERIN, J.A. FLECK, B.D. DOWNING & B.A. BERGAMASCHI. 2016. Optical properties of dissolved organic matter (DOM): Effects of biological and photolytic degradation. *Limnology and Oceanography*, 61 (3): 1015–1032. DOI: 10.1002/lno.10270

HAYASE, K. & H. TSUBOTA. 1985. Sedimentary humic acid and fulvic acid as fluorescent organic materials. *Geochimica et Cosmochimica Acta*, 49 (1): 159–163. DOI: 10.1016/0016-7037(85)90200-5

HELMS, J.R., A. STUBBINS, J.D. RITCHIE, E.C. MINOR, D.J. KIEBER & K. MOPPER. 2008. Absorption spectral slopes and slope ratios as indicators of molecular weight, source, and photobleaching of chromophoric dissolved organic matter. *Limnology and Oceanography*, 53 (3): 955–969. DOI: 10.4319/lo.2008.53.3.0955

HUGUET, A., L. VACHER, S. RELEXANS, S. SAUBUSSE, J.M. FROIDEFOND & E. PARLANTI. 2009. Properties of fluorescent dissolved organic matter in the Gironde Estuary. *Organic Geochemistry*, 40 (6): 706–719. DOI: 10.1016/j.orggeochem.2009.03.002

JUNK, W., P.B. BAYLEY & R.E. SPARKS. 1989. The Flood Pulse Concept in River-Floodplain Systems. D.P. Dodge, ed. Proceedings of the International Large River Symposium (LARS). *Canadian Special Publication of Fisheries and Aquatic Sciences*, 106: 110-127

KAUSHAL, S.S., W.H. MCDOWELL & W.M. WOLLHEIM. 2014. Tracking evolution of urban biogeochemical cycles: past, present, and future. *Biogeochemistry*, 121 (1): 1–21. DOI: 10.1007/s10533-014-0014-y

KEIL, R. & D. KIRCHMAN. 1991. Contribution of dissolved free amino acids and ammonium to the nitrogen requirements of heterotrophic bacterioplankton. *Marine Ecology Progress Series*, 73: 1–10. DOI: 10.3354/meps073001

LAKOWICZ, J.R. 2006. Principles of Fluorescence Spectroscopy. *Analytical and Bioanalytical chemistry*, 390 (5): 1223-1224. DOI: 10.1007/s00216-007-1822-x

LAUDON, H. & O. SLAYMAKER. 1997. Hydrograph separation using stable isotopes, silica and electrical conductivity: an alpine example. *Journal of Hydrology*, 201 (1): 82–101. DOI: 10.1016/S0022-1694(97)00030-9

LAWAETZ, A.J. & C.A. STEDMON. 2009. Fluorescence Intensity Calibration Using the Raman Scatter Peak of Water. *Applied Spectroscopy*, 63 (8): 936–940. DOI: 10.1366/000370209788964548

LEENHEER, J.A. 2009. Systematic approaches to comprehensive analyses of natural organic matter. *Annals of Environmental Science*, 3: 1–130.

MANN, H.B. & D.R. WHITNEY. 1947. On a Test of Whether one of Two Random Variables is Stochastically Larger than the Other. *The Annals of Mathematical Statistics*, 18 (1): 50–60.

MARANGER, R.J., M.L. PACE, P.A. del GIORGIO, N.F. CARACO & J.J. COLE. 2005. Longitudinal Spatial Patterns of Bacterial Production and Respiration in a Large

River–Estuary: Implications for Ecosystem Carbon Consumption. *Ecosystems*, 8 (3): 318–330. DOI: 10.1007/s10021-003-0071-x

MASSEY, F.J. 1951. The Kolmogorov-Smirnov Test for Goodness of Fit. *Journal of the American Statistical Association*, 46 (253): 68–78. DOI: 10.1080/01621459.1951.10500769

MEYBECK, M. 1982. Carbon, nitrogen, and phosphorus transport by world rivers. *American Journal of Science*, 282 (4): 401–450. DOI: 10.2475/ajs.282.4.401

MURPHY, J. & J.P. RILEY. 1962. A modified single solution method for the determination of phosphate in natural waters. *Analytica Chimica Acta*, 27: 31–36. DOI: 10.1016/S0003-2670(00)88444-5

OHNO, T. 2002. Fluorescence Inner-Filtering Correction for Determining the Humification Index of Dissolved Organic Matter. *Environmental Science & Technology*, 36 (4): 742–746. DOI: 10.1021/es0155276

RAYMOND, P.A., J.E. SAIERS & W.V. SOBCZAK. 2016. Hydrological and biogeochemical controls on watershed dissolved organic matter transport: pulse-shunt concept. *Ecology*, 97 (1): 5–16. DOI: 10.1890/14-1684.1

REARDON, J. 1969. Salicylate method for the quantitative determination of ammonia nitrogen. U.S. Patent 3,432,395

ROUSSEEUW, P.J. 1987. Silhouettes: A graphical aid to the interpretation and validation of cluster analysis. *Journal of Computational and Applied Mathematics*, 20: 53–65. DOI: 10.1016/0377-0427(87)90125-7

SAADI, I., M. BORISOVER, R. ARMON & Y. LAOR. 2006. Monitoring of effluent DOM biodegradation using fluorescence, UV and DOC measurements. *Chemosphere*, 63 (3): 530–539. DOI: 10.1016/j.chemosphere.2005.07.075

SCHLESINGER, W.H. & J.M. MELACK. 1981. Transport of organic carbon in the world's rivers. *Tellus*, 33 (2): 172–187. DOI: 10.1111/j.2153-3490.1981.tb01742.x

THURMAN, E.M. 1985. Aquatic Humic Substances. In: *Organic Geochemistry of Natural Waters*. Developments in Biogeochemistry, vol 2. Springer Netherlands. Dordrecht. DOI: 10.1007/978-94-009-5095-5_11

VANNOTE, R.L., G.W. MINSHALL, K.W. CUMMINS, J.R. SEDELL & C.E. CUSHING. 1980. The River Continuum Concept. *Canadian Journal of Fisheries and Aquatic Sciences*, 37 (1): 130–137. DOI: 10.1139/f80-017

VÁZQUEZ, E., A.M. ROMANÍ, F. SABATER & A. BUTTURINI. 2007. Effects of the Dry–Wet Hydrological Shift on Dissolved Organic Carbon Dynamics and Fate Across Stream–Riparian Interface in a Mediterranean Catchment. *Ecosystems*, 10 (2): 239–251. DOI: 10.1007/s10021-007-9016-0

VÁZQUEZ, E., E. EJARQUE, I. YLLA, A.M. ROMANÍ & A. BUTTURINI. 2015. Impact of drying/rewetting cycles on the bioavailability of dissolved organic matter molecular-weight fractions in a Mediterranean stream. *Freshwater Science*, 34 (1): 263–275. DOI: 10.1086/679616

VICENTE-SERRANO, S.M., J.-I. LOPEZ-MORENO, S. BEGUERÍA, J. LORENZO-LACRUZ, ARTURO SANCHEZ-LORENZO, J.M. GARCÍA-RUIZ, C. AZORIN-MOLINA, E. MORÁN-TEJEDA, J. REVUELTO, RICARDO TRIGO, F. COELHO & F. ESPEJO. 2014. Evidence of increasing drought severity caused by temperature rise in southern Europe. *Environmental Research Letters*, 9 (4): 44001. DOI: 10.1088/1748-9326/9/4/044001

WEISHAAR, J.L., G.R. AIKEN, B.A. BERGAMASCHI, M.S. FRAM, R. FUJII & K. MOPPER. 2003. Evaluation of Specific Ultraviolet Absorbance as an Indicator of the Chemical Composition and Reactivity of Dissolved Organic Carbon. *Environmental Science & Technology*, 37 (20), 4702-4708. DOI: 10.1021/es030360x

WETZEL, R.G. 1992. Gradient-dominated ecosystems: sources and regulatory functions of dissolved organic matter in freshwater ecosystems. In: *Dissolved Organic Matter in Lacustrine Ecosystems*. K. Salonen, T. Kairesalo, and R. I. Jones (eds.): 181–198. Springer Netherlands. DOI: 10.1007/978-94-011-2474-4_14

WILCOXON, F. 1945. Individual Comparisons by Ranking Methods. *Biometrics Bulletin*, 1 (6): 80–83. DOI: 10.2307/3001968

WOLLHEIM, W.M., R.J. STEWART, G.R. AIKEN, K.D. BUTLER, N.B. MORSE & J. SALISBURY. 2015. Removal of terrestrial DOC in aquatic ecosystems of a temperate river network. *Geophysical Research Letters*, 42 (16): 2015GL064647. DOI: 10.1002/2015GL064647

Con el apoyo de:

GOBIERNO DE ESPAÑA
MINISTERIO PARA LA TRANSICIÓN ECOLÓGICA
Fundación Biodiversidad